

# Determination of the glass transition temperature of polymer/layered silicate nanocomposites from positron annihilation lifetime measurements

Sung Ho Kim<sup>a</sup>, Jae Woo Chung<sup>a</sup>, Tae Jin Kang<sup>a</sup>, Seung-Yeop Kwak<sup>a,\*</sup>, Takenori Suzuki<sup>b</sup>

<sup>a</sup> School of Materials Science and Engineering, Seoul National University, San 56-1, Sillim-dong, Gwanak-gu, Seoul 151–744, Republic of Korea

<sup>b</sup> Radiation Science Center, High Energy Accelerator Research Organization (KEK), Tsukuba, Ibaraki 305-0801, Japan

Received 6 November 2006; received in revised form 3 May 2007; accepted 4 May 2007

Available online 13 May 2007

## Abstract

The glass transitions of acrylonitrile–butadiene rubber (NBR)/organoclay nanocomposites with various silicate contents were investigated using positron annihilation lifetime spectroscopy (PALS). The nanocomposites were prepared through melt intercalation of NBR with various concentrations of organoclay (OC30B) modified with the organic modifier, methyl tallow bis(2-hydroxyethyl) quaternary ammonium (MT2EtOH), i.e., Cloisite<sup>®</sup> 30B. X-ray diffraction (XRD) and high-resolution transmission electron microscopy (HR-TEM) measurements of the NBR/OC30B nanocomposites showed that the NBR chains were intercalated between the silicate layers, thereby increasing the gallery heights of the organosilicates. The glass transition temperature of NBR was determined using differential scanning calorimetry (DSC). However, it seemed to be very difficult to clearly resolve the very small differences in  $T_g$ s caused from various loading of nanosized silicate in NBR/OC30B nanocomposites. Hence, we performed positron annihilation lifetime spectroscopy (PALS) on NBR/OC30B nanocomposites containing various amounts of OC30B (1–10 wt%). Significant changes in the temperature dependencies of free volume parameters (i.e., lifetimes and intensities) were observed at the transition temperature,  $T_{g,PALS}$ , and the  $T_{g,PALS}$  values were found to increase with increasing organoclay content in the samples. These observations are consistent with PALS having a higher sensitivity in the detection of very small changes in free volume properties. The present findings thus highlight the usefulness of PALS for studying phase transition phenomena in polymeric materials with nanoscale structural variations. © 2007 Elsevier Ltd. All rights reserved.

**Keywords:** Positron annihilation lifetime spectroscopy (PALS); Polymer/layered silicate nanocomposite; Glass transition temperature

## 1. Introduction

Polymer/layered silicate nanocomposites have received much attention due to their markedly improved mechanical, thermal, optical, and physico-chemical properties compared to pure polymer or conventional microscale composites, since the concept was introduced by researchers at Toyota Central Research and Development Laboratories at the late 1980s [1–3]. These improvements, which include increases in moduli, swelling resistance, and ionic conductivity, and decreases in thermal expansion coefficient and gas permeability, presumably derive from the nanoscale structure of the layered silicates in the form of sheets one to a few nanometers thick and hundreds to thousands of nanometers long. Various

polymer/layered silicate nanocomposites, involving thermoplastic and thermosetting resins, and recently thermoplastic and thermoset rubbers, have been reported recently [4–8]. Several strategies have been proposed to prepare polymer/layered silicate nanocomposites, including exfoliation–adsorption, in situ intercalative polymerization, melt intercalation, and template synthesis. Among them, the melt intercalation method is considered to be useful for commercial production because it does not require a solvent. When the polymer molecules are intercalated between two parallel solid surfaces separated by 1.5–2.0 nm, the confined environments will affect the relaxation behaviors of the polymer segments and behavior of polymers [2,9].

Polymers exhibit various physical and mechanical behaviors, depending on the temperature. At low temperatures, polymers are glassy, hard, and brittle. As the temperature is increased, however, they undergo a phase transition, known

\* Corresponding author. Tel.: +82 2 880 8365; fax: +82 2 885 1748.

E-mail address: [sykwak@snu.ac.kr](mailto:sykwak@snu.ac.kr) (S.-Y. Kwak).

as the glass–rubber transition, which is accompanied by drastic changes in their properties. The glass transition is the most important thermal transition that a polymer undergoes. At the glass transition temperature,  $T_g$ , the polymer softens due to the onset of long-range coordinated molecular motion accompanied by a change in the free volume properties in the polymer. Differential scanning calorimetry (DSC) is one of the most widely used techniques for evaluating cooperative motion of polymer segments. However, the relatively low sensitivity of DSC restricts its usefulness.

The molecular mobility highly depends on the available free volume, which plays an important role in deciding the mechanical properties, diffusion of small molecules through the polymer and so on. Thus, some studies on free volume properties of nanocomposites were carried out with some theoretical calculation and experimental techniques. Utracki et al. investigated pressure–volume–temperature (PVT) behaviors of several polymer/clay nanocomposites such as poly- $\epsilon$ -caprolactam (PA6)/clay, polystyrene (PS)/clay with a Gnomix dilatometer and theoretical calculation [10–12]. They reported that incorporation of 1.6 wt% clay reduced the free volume fraction by 14% in PA6/clay, while only a 5% volume reduction was observed in the PS nanocomposites containing 4 wt%. Although they showed that the total fraction of free volume in nanocomposites could depend on the type of polymers used for the sample preparation, the PVT measurement of averaged specific volume in samples cannot give any detailed information about sizes and numbers of molecular-sized free volume sites. There is another important study that the free volume properties of nanocomposites can depend not only on the type of polymers used but also sample preparation method. Wang et al. applied positron annihilation lifetime spectroscopy (PALS) for the study on the effect of dispersion state of silicate on the free volume characteristics of styrene–butadiene rubber (SBR)/clay nanocomposites prepared by both latex compounding and melt blending [13]. Maurer et al. also demonstrated the importance of PALS for the polymer/clay nanocomposites from the study correlating free cavity size with thermal and viscoelastic properties of nanocomposites [14]. The PALS is regarded as a unique technique that directly probes the molecular-level free volume cavities by measuring the positron and/or positronium lifetimes in samples [15,16]. Given that the molecular mobility depends on the available free volume, PALS measurements have been used to characterize phase transition phenomena in polymers [17,18]. However, the research to directly correlate the change in free volume properties with glass transition temperature of nanocomposites in conjunction with the correlation of silicate loading on the transition is less reported in the literature, despite the importance of the study for the scientific exploration and also for the use of nanocomposites in engineering applications.

In the present study, we prepared acrylonitrile–butadiene rubber (NBR)/organoclay (OC30B $x$ ) nanocomposites containing  $x$  wt% of organoclay modified with the polar intercalant, methyl tallow bis(2-hydroxyethyl) quaternary ammonium. NBR is one of the most widely used elastomers in several engineering applications due to its excellent chemical and

thermal stabilities. Recognizing that the glass transition temperature,  $T_g$ , is the most important parameter in polymers, DSC and PALS measurements were performed to analyze changes in the thermal behavior of the intercalated NBR/OC30B nanocomposites. The main objective of this study is to investigate the temperature dependent relaxation behaviors of free volume properties in NBR/OC30B nanocomposites and the effects of their nanosized organoclay contents on the glass transition temperatures.

## 2. Experimental section

### 2.1. Materials

Acrylonitrile–butadiene rubber (NBR), containing approximately 34 wt% acrylonitrile was supplied by Korea Kumho Petrochemical Co., Ltd. The glass transition temperature,  $T_g$ , of the NBR is about  $-25^\circ\text{C}$  according to the supplier. The clay used in this study was Cloisite<sup>®</sup> 30B (OC30B) of Southern Clay Products, which was a natural montmorillonite modified with an organic modifier, methyl tallow bis(2-hydroxyethyl) quaternary ammonium (MT2EtOH) as shown in Fig. 1. Tallow is composed of 65 wt% C<sub>18</sub>, 30 wt% C<sub>16</sub>, and 5 wt% C<sub>14</sub>. The cationic exchange capacity (CEC) and interlayer gallery height of OC30B are given by the manufacturer as 90 meq/100 g and 0.94 nm, respectively.

### 2.2. Preparation of nanocomposites

NBR/organoclay (OC30B $x$ ) nanocomposites containing  $x$  wt% of organoclay were fabricated with a Haake Rheocord 600P internal mixer using banbury blades operating at a rotor speed of 100 rpm and a fill factor of 0.7. The NBR was first masticated at  $65^\circ\text{C}$  for 30 s, then mixed with organoclay at  $90^\circ\text{C}$  for 600 s and annealed for 100 min at the same temperature. The compositions of NBR/OC30B $x$  nanocomposites are shown in Table 1.

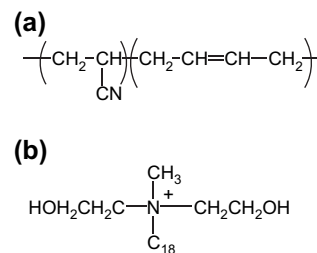


Fig. 1. Chemical structures of acrylonitrile–butadiene rubber (NBR) (a) and methyl tallow bis(2-hydroxyethyl) quaternary ammonium (MT2EtOH) (b).

Table 1  
Compositions of the NBR/organoclay nanocomposites

Sample	NBR (wt%)	Intercalant (wt%)	Montmorillonite (wt%)
NBR/OC30B1	98.6	0.4	1
NBR/OC30B5	92.8	2.2	5
NBR/OC30B10	85.6	4.4	10

### 2.3. X-ray diffraction analyses (XRD) and transmission electron microscopy

X-ray diffraction (XRD) analyses were used to characterize change in the internal spacing of the organoclay in the nanocomposites. The XRD analyses were performed using a MAC Science MXP 18A-HF X-ray diffractometer with Cu K $\alpha$  radiation ( $\lambda = 0.154$  nm) operated at 40 kV and 100 mA. The diffraction patterns were collected between 1° and 12° at a scanning rate of 3°/min. The spacing,  $d$ , of clay layers was determined from the (001) peak using Bragg's law:  $d = \lambda/2 \sin \theta_{\max}$ .

High-resolution transmission electron microscopic (HR-TEM) analysis was performed with a Jeol JEM 3010CX at 300 kV. For the TEM observations, ultra-thin cross-sections of the specimens were prepared by using a Leica Ultracut UCT ultracycromicrotome.

### 2.4. Differential scanning calorimetry (DSC)

Differential scanning calorimetry (DSC) was performed with a TA instruments DSC 2920 under a nitrogen atmosphere. The samples were first heated to 120 °C, maintained at that temperature for 5 min and then quenched to -100 °C to remove the thermal history. Then, a second scan was carried out from -100 to 60 °C at a heating rate of 10 °C/min. The glass transition temperatures,  $T_g$ , of the samples were determined from the midpoints of the transitions.

### 2.5. Positron annihilation lifetime spectroscopy (PALS)

Positron annihilation experiments were performed using a fast–fast coincidence system under vacuum. The  $^{22}\text{Na}$  positron source was prepared by depositing about 3.7 MBq of  $^{22}\text{NaCl}$  on a 7  $\mu\text{m}$  thick Kapton foil of 1  $\text{cm}^2$  and being covered with another foil of the same size. The diameter of the deposit was 1–1.5 mm. The sample–source in a sandwich geometry was fixed on the cooling finger of a helium cryostat (CW303, Iwatani Planech Co.), and the temperature was controlled by a temperature control device (TCU-4, Iwatani Plantech Co.). The samples were first cooled down to 30 K from RT over about 1 h, maintained at that temperature for several hours and then heated at a rate of about 5  $\text{K h}^{-1}$ . The measurement was performed in the temperature range of 30–370 K. Each positron annihilation lifetime spectrum was automatically collected every 1 h, resulting in 1–2 million events in each spectrum. The lifetime spectra were resolved into three components using the PATFIT program.

## 3. Results and discussion

### 3.1. X-ray diffraction analysis and transmission electron microscopy

Fig. 2 shows the XRD spectra of OC30B and NBR/OC30B $_x$  nanocomposites with various organoclay contents. The OC30B exhibits the (001) peak at  $2\theta$  of 4.76°, which

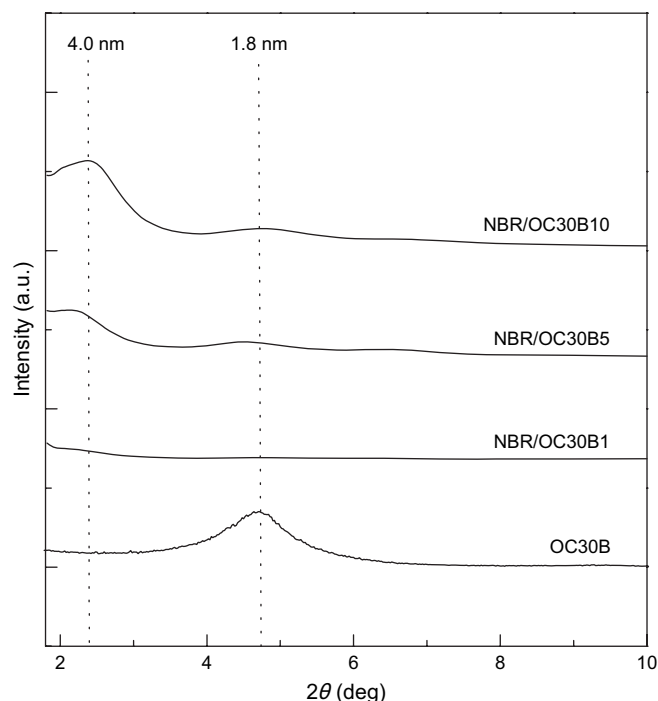


Fig. 2. X-ray diffraction patterns for organoclay (OC30B) and polymer-layered silicates nanocomposites (NBR/OC30B $_x$ ) with various silicate contents.

corresponds to a basal lattice spacing of 18 Å. This peak shifts to smaller angle in the spectra of the NBR/OC30B $_x$  samples, indicating that the gallery heights of the organosilicates increases during the preparation of the nanocomposites. The intergallery heights of NBR/OC30B nanocomposites after intercalation are found to be approximately 40 Å from the XRD results. Thus, the interlayer gallery heights of NBR/OC30B $_x$  are increased by about 22 Å with respect to those of pristine OC30B. Fig. 3 displays a HR-TEM image of NBR/OC30B $_x$  nanocomposite. Individual crystallites of the silicate are visible as regions of alternating narrow, dark and light bands within the fringes. Intercalated nanocomposites, similar to

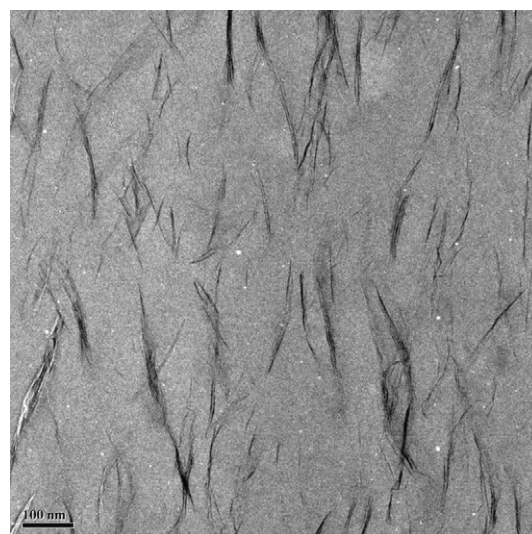


Fig. 3. HR-TEM micrograph of NBR/OC30B $_x$  nanocomposite (at  $x = 5$ ).

unintercalated layered silicates, exhibit the microstructure depicted in Fig. 3, with the only difference being an expansion of the gallery height to accommodate the intercalated polymer. Thus, the combined consideration with XRD and TEM results of Figs. 2 and 3 indicates that the polymer chains were sandwiched in-between silicate layers, namely intercalated nanocomposites, were successfully obtained from melt mixing of NBR with OC30B.

### 3.2. Differential scanning calorimetry (DSC)

The glass transition temperature,  $T_g$ , of a polymer is an important indicator of its thermal properties. Fig. 4 shows the DSC thermograms of NBR and the NBR/OC30B $x$  nanocomposites containing various amounts of OC30B (1–10 wt%). All of the samples have  $T_g$  values of approximately  $-25^\circ\text{C}$ . As shown in the figure, it is very difficult to clearly discern the differences in the  $T_g$  only on the DSC data. Therefore, we turned to the PALS method to evaluate the structural change in the nanocomposites as a function of silicate loadings.

### 3.3. Positron annihilation lifetime spectroscopy (PALS)

Positron annihilation lifetime spectroscopy (PALS) is a unique technique that measures lifetimes of positrons in polymer samples and characterizes their free volume hole properties. When positrons emitted from a  $^{22}\text{Na}$  radioisotope source are injected into a polymer, they either (i) diffuse into the media and become annihilated as a free positron with a free electron (free positron annihilation) or (ii) capture an electron from the material and form a bound-state positronium (Ps) of two spin states, i.e., *para*-Ps (*p*-Ps) with an anti-parallel spin state or *ortho*-Ps (*o*-Ps) with a parallel spin state. Thus, three components are usually obtained in the samples. The first component ( $\tau_1 \sim 0.15$  ns) is related to the positron annihilation of *p*-Ps with the shortest lifetime. The second component

( $\tau_2 \sim 0.3\text{--}0.5$  ns) is due to the annihilation of free positrons. The third long-lived component ( $\tau_3 \sim$  a few ns) is associated with annihilation of *o*-Ps in the molecular-level space of polymer structure [15,16].

*o*-Ps parameters, including the *o*-Ps lifetime,  $\tau_{o\text{-Ps}}$ , and its intensity,  $I_{o\text{-Ps}}$ , have been shown to be highly correlated with properties of molecular-level free space (radius,  $R$  of  $\sim \text{\AA}$ ) in polymers. The *o*-Ps lifetime is related to the radius of free volume holes in samples; the longer the lifetime of *o*-Ps, the larger the  $R$ , and vice versa, as follows [16]:

$$\tau_{o\text{-Ps}} = \frac{1}{2} \left[ 1 - \frac{R}{R_0} + \frac{1}{2\pi} \sin\left(\frac{2\pi R}{R_0}\right) \right]^{-1} \quad (1)$$

where  $\tau_{o\text{-Ps}}$  is the *o*-Ps lifetime (ns),  $R$  is the radius ( $\text{\AA}$ ) of free hole space, and  $R_0$  is  $R + \Delta R$  where the fitted empirical electron layer thickness  $\Delta R$  is  $1.66 \text{ \AA}$ . The intensity is found to be related to the number of free volume hole sites if no Ps-quenching functional groups exist in the molecular structure of the polymer. There are some reports that results of PAL measurement in polymers (i.e., the values of *o*-Ps components) depend on the crystallinity, degree of cross-linking, polymer

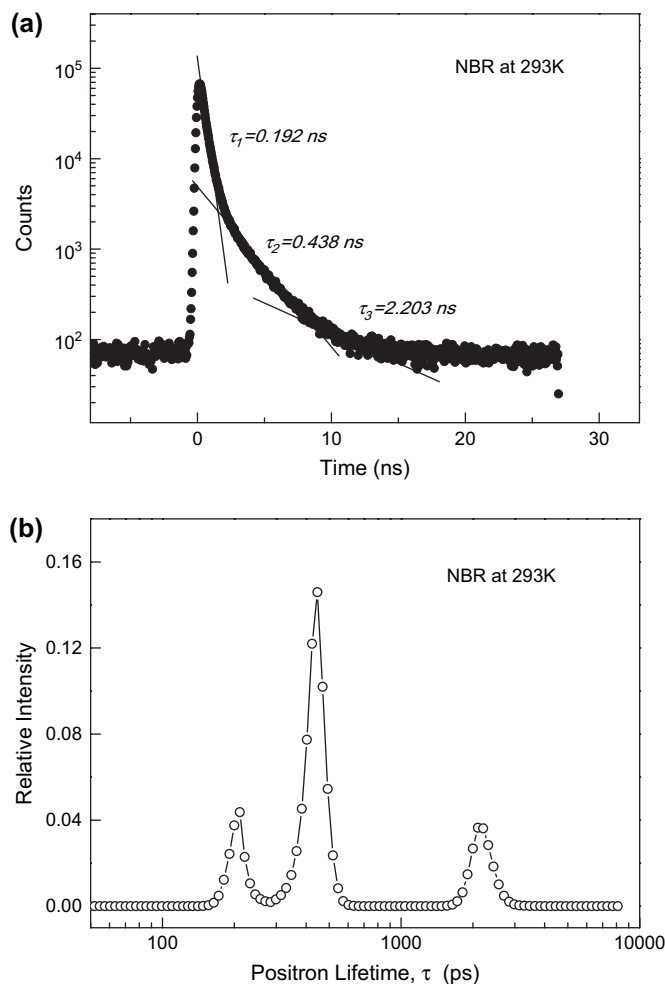


Fig. 5. Positron annihilation decay curve (a) and lifetime distribution (b) of NBR at 293 K.

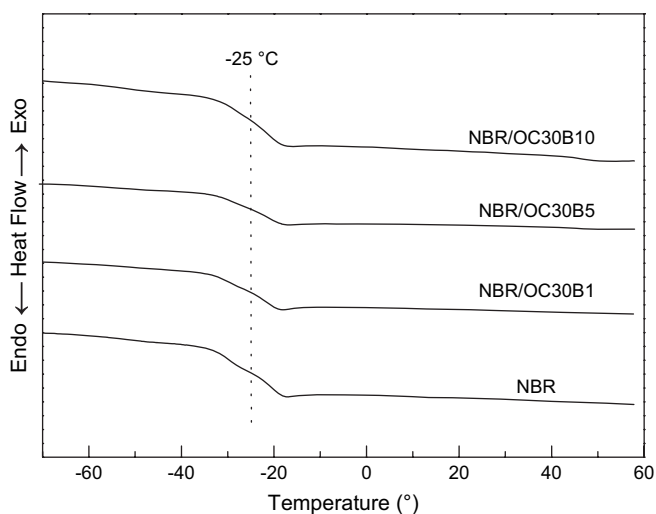


Fig. 4. DSC thermograms of NBR and NBR/OC30B $x$  with various silicate contents.

structure, polymerization, and so on. In this study, the dependencies of  $\tau_3$  and  $I_3$  on temperatures are used as parameters for the discussion of relaxation behavior of polymer structures.

A typical spectrum of positron annihilation for pure NBR at 293 K is shown in Fig. 5(a). The decay curve of positron annihilation in the sample was first analyzed through a continuous lifetime analysis using the maximum entropy lifetime (MELT) program [19,20]. The lifetime distribution of pure NBR at 273 K exhibits three well-defined peaks, as shown in Fig. 5(b). The discrete averages of *o*-Ps lifetimes and intensities as a function of temperature were then resolved into three components through PATFIT analysis [21], as represented in the Fig. 5(a). The results obtained in the PATFIT analysis are in good agreement with those of the MELT analysis of Fig. 5(b). The positron lifetime spectra for NBR and NBR/OC30B nanocomposites could be well-resolved into three components. The lifetimes and intensities of the third lifetime components for pure NBR at various temperatures are shown in Fig. 6(a). The slope of the  $\tau_{o\text{-Ps}}$ –temperature curve for NBR increases significantly at 237.5 K, which can be attributed to a greater rate of increase of the free volume with temperature as the molecular motions of the polymer chains become more vigorous. The glass transition temperature determined from PALS experiment,  $T_{g,\text{PALS}}$ , is lower than the  $T_g$  determined by DSC measurement as has often been observed previously [15]. This discrepancy may be due to the longer duration of

the PAL measurement at one temperature compared to DSC. The variation in *o*-Ps intensities,  $I_{o\text{-Ps}}$ , with temperatures for NBR seems to be more complex than that of  $\tau_{o\text{-Ps}}$ . The  $I_{o\text{-Ps}}$  increases in the temperature range below  $T_{g,\text{PALS}}$ , and then flattens out above  $T_{g,\text{PAL}}$ . These results suggest that the glass transition for NBR involves an increase in hole size rather than number of holes.

The temperature dependences of the *o*-Ps lifetimes and their intensities for NBR/OC30B $x$  nanocomposites with various organoclay contents are shown in Fig. 6(b)–(d). Inflection points are observed in the  $\tau_{o\text{-Ps}}$ –temperature curves for NBR/OC30B $x$ , and their *o*-Ps intensities exhibit temperature dependencies similar to those of pure NBR. From these relaxation behaviors of positron lifetimes in the nanocomposites, we can determine the transition temperatures,  $T_{g,\text{PALS}}$ , for the samples. The  $T_{g,\text{PALS}}$  values are found to increase with increases in the organoclay content in the samples. This trend stands in contrast to the findings based on conventional DSC measurements, which indicates similar  $T_g$  values for all nanocomposites. The discrepancy between DSC and PALS findings can be attributed to the differences in sensitivities of the two methods. DSC is a very useful technique for evaluating cooperative motion of polymer segments on a scale of 10–30 nm, whereas the PALS is based on the sensitivity of the *o*-Ps probe and hence can detect very small changes in free volume properties ranging from 0.1 to 2 nm. The present findings thus

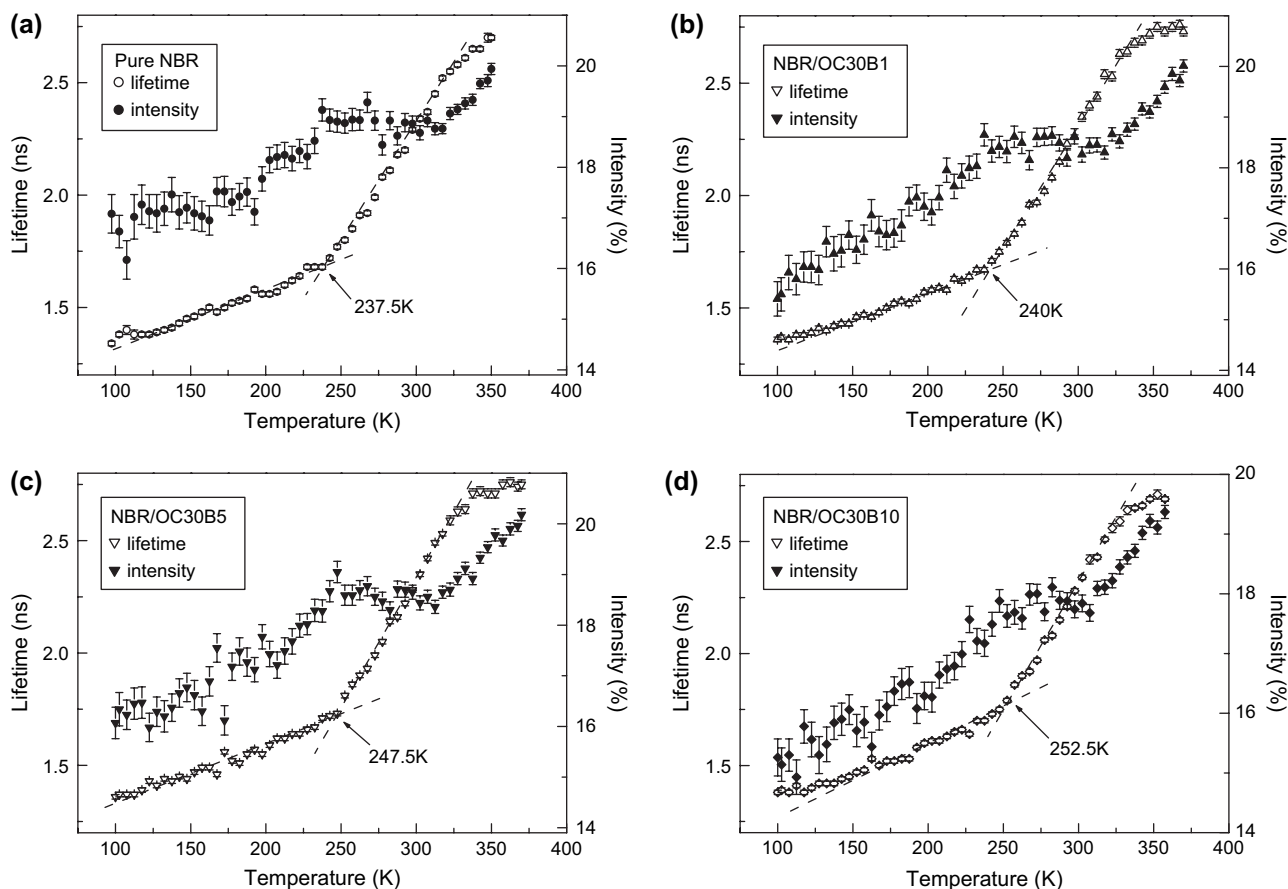


Fig. 6. *o*-Ps lifetime,  $\tau_3$ , and intensity,  $I_3$ , for NBR and NBR/OC30B nanocomposites with various silicate contents as a function of temperature.

Table 2  
*o*-Ps lifetimes, intensities, radii, and fractional free volumes of NBR and NBR/OC30B nanocomposites at room temperature

Sample	$\tau_{o\text{-Ps}}$ (ns)	$I_{o\text{-Ps}}$ (%)	$R$ (Å)	$V_f \times I_{o\text{-Ps}}$	$f_v$
NBR	$2.29 \pm 0.01$	$18.86 \pm 0.15$	3.11	2380	0.354
NBR/OC30B1	$2.26 \pm 0.01$	$18.62 \pm 0.15$	3.09	2300	0.343
NBR/OC30B5	$2.28 \pm 0.01$	$18.65 \pm 0.14$	3.10	2330	0.347
NBR/OC30B10	$2.28 \pm 0.01$	$17.74 \pm 0.14$	3.10	2210	0.330

highlight the usefulness of PALS for studying phase transition phenomena in polymeric materials with nanoscale structural variations.

The free volume fraction of a polymer system,  $f_v$ , is given by the following equation [22]:

$$f_v \equiv V_f C_f = V_f (A I_{o\text{-Ps}} + B) \cong A V_f I_{o\text{-Ps}} \quad (2)$$

where  $V_f (=4/3\pi R^3)$  is the hole volume determined from the *o*-Ps lifetime using Eq. (1),  $C_f$  is the hole concentration, and  $I_3$  is the *o*-Ps intensity.  $A$  and  $B$  are constants, which may be determined from specific volume data. In this study, the value of  $A$  was determined from the relation of the bulk density of pure NBR ( $=0.98$ ) with its theoretical van der Waals volume and further used for evaluation of the free volume fractions of pure NBR and NBR/OC30B $x$  nanocomposites. The bulk density,  $\rho_{\text{bulk}}$ , is related to the structural unit contribution and free volume, as follows:

$$\rho_{\text{occ}} \times (1 - f_v) + \rho_f \times f_v = \rho_{\text{bulk}} \times 1$$

$$\rho_{\text{occ}} \times (1 - A V_f I_{o\text{-Ps}}) = \rho_{\text{bulk}} \quad (\because \rho_{\text{occ}} \gg \rho_f \approx 0) \quad (3)$$

where the occupied volume density,  $\rho_{\text{occ}}$ , of pure NBR was obtained from group contribution of mass and van der Waals volume according to Bondi [23,24]. Table 2 summarizes the measured *o*-Ps lifetimes,  $\tau_{o\text{-Ps}}$ , the intensities,  $I_{o\text{-Ps}}$ , the calculated radii,  $R$ , of free volume cavities, relative fractional free volume,  $V_f \times I_{o\text{-Ps}}$ , and the fractional free volume,  $f_v$ , of samples at room temperature. It shows that the organoclay intercalation caused a slight reduction in total free volume fraction of the resulting nanocomposites with no significant change in the size of free volume cavity. About 2.4 wt% of reduction in free volume fraction was observed in the NBR/OC30B10 as compared with pure NBR.

#### 4. Conclusions

Positron annihilation lifetime spectroscopy (PALS) was used as a novel tool to investigate the glass–rubber transition of polymer/layered silicate nanocomposites with various silicate contents.

(1) Acrylonitrile–butadiene rubber (NBR)/organoclay (OC30B $x$ ) nanocomposites containing  $x$  wt% of organoclay modified with polar intercalant were fabricated by melt intercalation. X-ray diffraction and HR-TEM analyses showed that the NBR chains were successfully melt intercalated within the silicate layers.

(2) The glass transition temperatures,  $T_g$ , of NBR/OC30B nanocomposites were first determined by DSC. The  $T_g$  of pure NBR was easily determined to be approximately  $-25$  °C, but it was very difficult to clearly distinguish the difference among the  $T_g$  values of the nanocomposites with various silicate loadings.

(3) Thus, the PALS study was used to study the nanocomposites with nanoscopic structural variations. Significant changes in the slopes of the  $\tau_{o\text{-Ps}}$ -temperature and  $I_{o\text{-Ps}}$ -temperature curves as the samples pass through the transition temperature,  $T_{g,\text{PALS}}$ . The values of  $T_{g,\text{PALS}}$  were found to increase with increasing organoclay content in the samples, and the effect of silicate loading on the total free volume fraction was investigated. This study demonstrated the great potential of PALS for studying phase transition phenomena in polymers with nanoscale structural variations.

#### Acknowledgement

The authors of this paper would like to thank the Korea Science and Engineering Foundation (KOSEF) for sponsoring this research through the SRC/ERC Program of MOST/KOSEF (R11-2005-065).

#### References

- [1] Alexandre M, Dubois P. Mater Sci Eng R 2000;28:1–63.
- [2] Vaia RA, Sauer BB, Tse OK, Giannelis EP. J Polym Sci Part B Polym Phys 1997;35:59–67.
- [3] Hwang W-G, Wei K-H, Wu C-M. Polymer 2004;45:5729–34.
- [4] Agar T, Koga T, Takeichi T. Polymer 2001;42:3399–408.
- [5] Tien YI, Wei KH. Macromolecules 2001;34:9045–52.
- [6] Manias EA, Touny L, Wu KE, Strawhecker BL, Chung TC. Chem Mater 2001;13:3516–23.
- [7] Vu YT, Mark JE, Phom LH, Engelhardt M. J Appl Polym Sci 2001;82:1391–403.
- [8] Karger-Kocsis J, Wu C-M. Polym Eng Sci 2004;44:1083–93.
- [9] Lu H, Nutt S. Macromolecules 2003;36:4010–6.
- [10] Simha R, Utracki LA, Garcia-Rejon A. Compos Interfaces 2001;8:345–53.
- [11] Utracki LA, Simha R, Garcia-Rejon A. Macromolecules 2003;36:2114–21.
- [12] Tanoue S, Utracki LA, Garcia-Rejon A, Tatibouet J, Cole KC, Kamal MR. Polym Eng Sci 2004;44:1046–60.
- [13] Wang Y-Q, Wu Y-P, Zhang H-F, Zhang L-Q, Wang B, Wang Z-F. Macromol Rapid Commun 2004;25:1973–8.
- [14] Winberg P, Eldrup M, Pedersen NJ, Van Es MA, Maurer FHJ. Polymer 2005;46:8239–49.
- [15] Jean YC, Mellon PE, Schrader DM. Principles and applications of positron and positronium chemistry. Singapore: World Scientific; 2003 [chapter 10].
- [16] Schrader DM, Jean YC. Positron and positronium chemistry. New York: Elsevier; 1988.

- [17] He C, Suzuki T, Ma L, Matsuo M, Shantarovich VP, Kondo K, et al. *Phys Lett A* 2002;304:49–53.
- [18] Suzuki T, He C, Shantarovich V, Kondo K, Ito Y, Matsuo M. *Mater Res Innovations* 2003;7:31–6.
- [19] Shukla A, Peter M, Hoffmann L. *Nucl Instrum Methods Phys Res Sect A* 1993;335:310–7.
- [20] Wastlund C, Maurer FHJ. *Nucl Instrum Methods Phys Res Sect B* 1996; 117:467–73.
- [21] Kirkegaard P, Eldrup M, Mogensen OE, Pedersen N. *Comput Phys Commun* 1981;23:307–35.
- [22] Nakanish H, Jeac YC. *J Polym Sci Part B Polym Phys* 1989;27: 1419–24.
- [23] Van Krevelen DW, Hoftyzer PJ. *Properties of polymers: their estimation and correlation with chemical structure*. New York: Elsevier; 1976.
- [24] Bondi A. *Physical properties of molecular crystals, liquids and glasses*. New York: Wiley; 1968.